Origin and Evolution of Oxygen Isotopic Compositions of the Solar System

Hisayoshi Yurimoto
Hokkaido University

Kiyoshi Kuramoto
Hokkaido University

Alexander N. Krot
University of Hawai'i at Manoa

Edward R. D. Scott
University of Hawai'i at Manoa

Jeffrey N. Cuzzi
NASA Ames Research Center

Mark H. Thiemens
University of California San Diego

James R. Lyons
University of California Los Angeles

On a three-isotope diagram oxygen isotopic compositions of most primitive meteorites (chondrites), chondritic components (chondrules, refractory inclusions, and matrix), and differentiated meteorites from asteroids and Mars deviate from the line along which nearly all terrestrial samples plot. Three alternative mechanisms have been proposed to explain this oxygen isotope anomaly: nucleosynthetic effects, chemical mass-independent fractionation effects, and photochemical self-shielding effects. Presently, the latter two are the most likely candidates for production of the isotopic anomalies. Recent data on solar wind oxygen isotopes lends support to the photochemical self-shielding scenario, but additional solar isotope data are needed. Observations, experiments and modeling are described that will advance our understanding of the complex history of oxygen in the solar system.

1. INTRODUCTION

Oxygen is the third most abundant element in the Solar System and the most abundant element of the terrestrial planets. The presence of oxygen in both gaseous and solid phases makes oxygen isotopes (the terrestrial abundance: ^{16}O = 99.757%, ^{17}O = 0.038%, and ^{18}O = 0.205%) important tracers of various fractionation processes in the solar nebula, which are essential for understanding the evolution of gaseous and solid phases in the early Solar System.

Oxygen isotopic compositions are normally expressed in δ units, which are deviations in part per thousand (permil, ‰) in the $^{17}O/^{16}O$ and $^{18}O/^{16}O$ ratios from Standard Mean Ocean Water (SMOW) with $^{17}O/^{16}O$ = 0.0003829 and $^{18}O/^{16}O$ = 0.0020052 (McKeegan and Leshin 2001): $\delta^{17,18}O_{SMOW} = [(^{17,18}O/^{16}O)_{sample}/(^{17,18}O/^{16}O)_{SMOW} - 1] \times 1000$. On a three-isotope diagram of $\delta^{18}O$ *vs.* $\delta^{17}O$, compositions of nearly all terrestrial samples plot along a single line of slope 0.52 called the terrestrial fractionation line. This line reflects *mass-dependent fractionation* from a single homogeneous source during chemical and physical

processes that results from differences in the masses of the oxygen isotopes. The slope 0.52 results from changes in $^{17}O/^{16}O$ that are nearly half those in $^{18}O/^{16}O$ because of isotopic mass differences; the precise value of the slope depends on the nature of the isotopic species or isotopologues (e.g., *Thiemens*, 2006). In contrast, O-isotopic compositions of the vast majority of extraterrestrial samples, including primitive (chondrites) and differentiated (achondrites) meteorites, deviate from the terrestrial fractionation line (Fig. 1; see section 4 for details), reflecting *mass-independent fractionation* processes that preceded accretion of these bodies in the protoplanetary disk. Samples from bodies that were largely molten and homogenized such as Mars and Vesta lie on lines that are parallel to the terrestrial fractionation line. Lunar samples show no detectable deviations from the terrestrial fractionation line, for reasons that are still debated (see section 8.4.3 for details). The deviation from the terrestrial fractionation line is commonly expressed as $\Delta^{17}O_{SMOW} = \delta^{17}O_{SMOW} - 0.52\times\delta^{18}O_{SMOW}$.

The origin of the O-isotopic variations or anomalies in solar system materials has been a major puzzle for planetary scientists since they were discovered over 30 years ago (*Clayton et al.*, 1973). The interpretation of the mass-independent O-isotopic variations or anomalies is one of the most important outstanding problems in cosmochemistry (*McKeegan and Leshin*, 2001). Here we discuss the nature of the O-isotopic anomalies in the solar system, the evolution of O-isotopic compositions in the solar nebula, and possible implications for other protoplanetary disks and planetary systems.

2. CHONDRITES AND THEIR COMPONENTS

Mass-independent oxygen isotopic variations were discovered in chondrites as their diverse components show effects that are much larger than those shown by bulk chondrites or achondrites (*Clayton et al.*, 1973). Chondritic meteorites consist of three major components, which may have formed at separate locations and/or times in the solar nebula: refractory inclusions [Ca,Al-rich inclusions (CAIs) and amoeboid olivine aggregates (AOAs)], chondrules, and fine-grained matrix (e.g., *Scott and Krot*, 2003). CAIs are ~1 μm to ~1 cm-sized irregularly-shaped or spheroidal objects composed mostly of oxides and silicates of calcium, aluminum, titanium, and magnesium. AOAs are physical aggregates of individual grains of forsterite (Mg_2SiO_4), Fe,Ni-metal, and small CAIs. Evaporation and condensation appear to have been the dominant processes during formation of

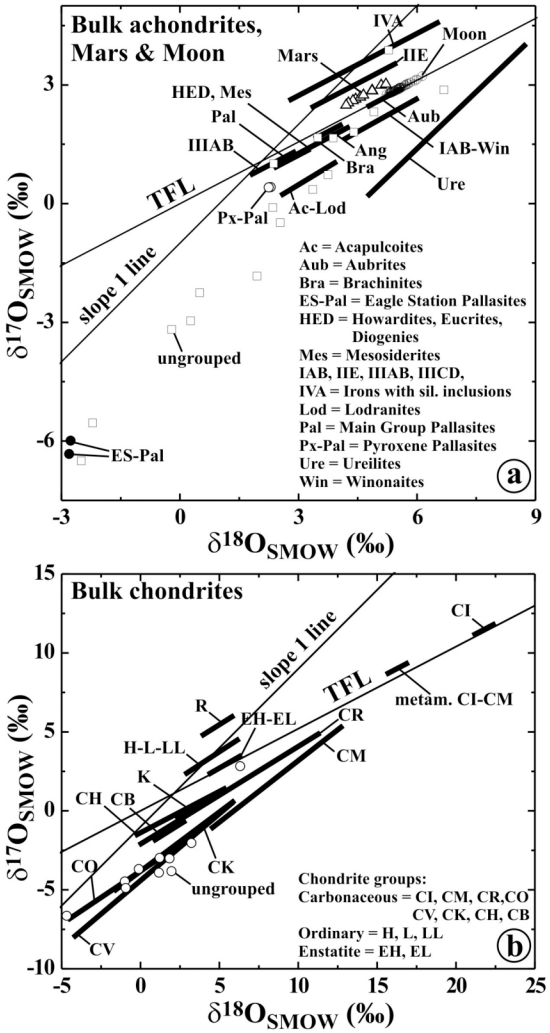

Fig. 1. Bulk O-isotopic compositions of achondrites and meteorites from Mars and Moon (**a**) and chondrites (**b**). Each group of meteorites probably represents a single asteroidal or planetary body. O-isotopic compositions of most meteorites deviate from the terrestrial fractionation line (TFL). Data from *Clayton and Mayeda* (1996, 1999).

refractory inclusions; subsequently some CAIs, called igneous CAIs, experienced extensive melting and partial evaporation (*MacPherson et al.*, 2005; *Wood*, 2004).

Chondrules are igneous, rounded objects, 0.01-10 mm in size, composed largely of crystals of ferromagnesian olivine ($Mg_{2-x}Fe_xSiO_4$) and pyroxene ($Mg_{1-x}Fe_xSiO_3$, where $1<x<0$) and Fe,Ni-metal with interstitial glassy or microcrystalline material. Most chondrules have textures that are consistent with crystal growth from a rapidly cooling (100-1000 K hr^{-1}) silicate melts (e.g., *Hewins et al.*, 2005). Some chondrules contain relict fragments of refractory inclusions and earlier generations of chondrules, and are surrounded by

igneous rims, suggesting chondrule formation was repetitive (e.g., *Jones et al.*, 2005, *Russell et al.*, 2005). Additionally, chondrules in primitive (unmetamorphosed) chondrites are often surrounded by fine-grained rims. Based on these observations, it is generally inferred that chondrules formed by varying degrees of melting of dense aggregates of ferromagnesian silicate, metal and sulfide grains during multiple flash-heating events, possibly by shock waves, in the dusty, inner (<5 AU) solar nebula (e.g., *Desch and Connolly*, 2002).

Matrix material is an aggregate of mineral grains, 10 nm – 5 μm in size, that surrounds refractory inclusions and chondrules and fills in the interstices between them. In primitive chondrites, matrix is made largely of magnesian olivine and pyroxene crystals, and amorphous ferromagnesian silicate particles (e.g., *Scott and Krot*, 2003). Matrices are chemically complementary to chondrules (*Brearley*, 1996), and may have largely experienced extensive evaporation and recondensation during chondrule formation (e.g., *Bland et al.*, 2005).

The ^{207}Pb-^{206}Pb absolute ages of CAIs from CV chondrites (4567.2 ± 0.6 Myr), and chondrules from the CV (4566.6 ± 1.0 Myr), ordinary (4566.3 ± 1.7 Myr), CR (4564.7 ± 0.6 Myr) and CB (4562.7 ± 0.5 Myr) chondrites indicate that chondrule formation started shortly after or maybe even contemporaneously with the CV CAIs and lasted for ~ 5 Myr (*Amelin et al.*, 2002; *Kita et al.*, 2005). We note, however, that chondrules in CB chondrites possibly formed from a vapor-melt plume caused by a giant impact between planetary embryos after the protoplanetary disk largely dissipated (*Krot et al.*, 2005a). Based on short-lived, ^{26}Al-^{26}Mg isotope chronology (see the chapter by *Wadhwa et al.*), it is inferred that most CAIs formed over a short period of time, perhaps only 0.3 Myr (*Bizzarro et al.*, 2004; *Young et al.*, 2005); some CAIs experienced late-stage remelting (*Krot et al.*, 2005c; *Russell et al.*, 2005).

The location of CAI and chondrule formation remains controversial. According to X-wind model, both components formed near the Sun and then were transported radially by X-wind where they accreted together with matrix into chondrite parent asteroids (e.g., *Itoh and Yurimoto*, 2003; *Shu et al.*, 2001; *Shu et al.*, 1996). Alternatively, chondrules and matrix formed in closed proximity to their accretion regions (e.g., *Jones et al.*, 2005), whereas refractory inclusions originated closer to the proto-Sun (*Cuzzi et al.*, 2003; *Scott and Krot*, 2003).

3. OXYGEN ISOTOPIC COMPOSITIONS OF CHONDRITIC COMPONENTS

CAIs, AOAs, and chondrules in primitive chondrites plot along a line of slope ~1 and show a large range of $\Delta^{17}O_{SMOW}$, from < -20‰ to +5‰ (e.g., *Aleon et al.*, 2002; *Clayton*, 1993; *Itoh et al.*, 2004). Within a chondrite group, AOAs and most CAIs are ^{16}O-rich relative to chondrules. Some igneous CAIs are ^{17,18}O-enriched to a level observed in chondrules (Fig. 2). Although matrix minerals show variations in O-isotopic compositions (e.g., *Kunihiro et al.*, 2005), their bulk O-isotopic compositions are probably similar to average compositions of chondrules [based on bulk O-isotopic compositions of chondrites (Fig. 1b), average O-isotopic compositions of chondrules, and abundance of matrix].

The observed variations in O-isotopic compositions of chondritic components are commonly explained as a result of mixing of ^{16}O-rich and ^{17,18}O-rich reservoirs in the solar nebula (e.g., *Clayton*, 1993).

The existence of an ^{16}O-rich gaseous reservoir in the inner solar nebula has been inferred from the ^{16}O-rich ($\Delta^{17}O_{SMOW}$ < -20‰) compositions of refractory solar nebula condensates, such as AOAs and fine-grained, spinel-rich CAIs with Group II rare earth element patterns (volatility-fractionated patterns indicating condensation from a gas from which more refractory rare earth elements have already been removed) (e.g., *Aleon et al.*, 2005a; *Krot et al.*, 2002; *Scott and Krot*, 2001).

The existence of an ^{17,18}O-rich gaseous reservoir in the inner solar nebula can be inferred from ^{17,18}O-rich compositions of chondrules, which probably experienced O-isotopic exchange with the nebular gas during chondrule melting events (*Krot et al.*, 2006; *Maruyama et al.*, 1999; *Yu et al.*, 1995), and from the ^{17,18}O-rich compositions of aqueously formed secondary minerals in chondrites (*Choi et al.*, 1998).

Because most solids in the inner solar system experienced thermal processing that could have modified their initial O-isotopic compositions, the bulk O-isotopic composition of solids in the proto-solar molecular cloud is unknown. Based on ^{16}O-rich compositions of the CAIs considered to be evaporative residues of the initial solar nebula dust (e.g., *Fahey et al.*, 1987; *Goswami et al.*, 2001; *Lee and Shen*, 2001; *Wood*, 1998), and from an ^{16}O-rich magnesian chondrule, which has been interpreted as a solidified melt of this dust (*Kobayashi et al.*, 2003), it is inferred that primordial solids in the proto-solar molecular cloud were ^{16}O-rich ($\Delta^{17}O_{SMOW}$ < -20‰) (*Itoh and Yurimoto*, 2003; *Scott and Krot*, 2001).

The chondrite matrix contains small amounts of silicate and oxide grains with grossly anomalous O-isotopic compositions that are inferred to have formed around massive stars (*Clayton and Nittler*, 2004). Silica grains with extremely high enrichments in ^{17}O and ^{18}O might have originated in a protostellar outflow

(*Aleon et al.*, 2005b). Only a small fraction of the presolar grains are ^{16}O-rich, and none of them plot along slope-1 line (*Nittler et al.*, 1998; *Nittler et al.*, 1997).

4. BULK OXYGEN ISOTOPIC COMPOSITIONS OF CHONDRITES AND ACHONDRITES

Bulk O-isotopic compositions of chondrites (Fig. 1b) show much smaller deviations from the terrestrial fractionation line than their components (Fig. 2) (*Clayton and Mayeda*, 1999). Most chondrite groups plot above or below the terrestrial fractionation line; the only exceptions are enstatite and CI carbonaceous chondrites (Fig. 1b). Chondrites in a single group define lines with slopes between 0.5 and 1 reflecting the mass-independent effects associated with their components as well as mass-dependent processes largely in their parent asteroids such as aqueous alteration and thermal metamorphism.

Bulk O-isotopic compositions of rocks from Mars and the Moon and achondrites tend to lie closer to the terrestrial fractionation line than the chondrites (Fig. 1a). Only aubrite (enstatite achondrite) and Moon samples lie on the terrestrial fractionation line. Samples from extensively melted bodies define lines that are parallel to the terrestrial fractionation line (e.g., angrites and HED meteorites from the asteroid Vesta), whereas meteorites from partly melted asteroids like the ureilites, acapulcoites, and winonaites define steeper lines as they were not homogenized during melting (*Greenwood et al.*, 2005).

5. OXYGEN ISOTOPIC COMPOSITION OF THE SUN

The oxygen isotopic composition of the Sun has not yet been measured directly. Oxygen isotopic compositions of solar wind implanted into the outermost (from two to a few hundred nanometers) surface layers of metal grains in the lunar regolith have been recently reported by *Hashizume and Chaussidon* (2005) and by *Ireland et al.* (2005). The measurements of *Hashizume and Chaussidon* (2005) revealed the presence of an ^{16}O-rich component with $\Delta^{17}O_{SMOW} < -20 \pm 4‰$, that was interpreted as the O-isotopic composition of the solar wind, and, hence, of the Sun, consistent with the earlier predictions of *Clayton* (2002), *Yurimoto and Kuramoto* (2004), *Krot et al.* (2005b), and *Lyons and Young* (2005). In contrast, the O-isotopic compositions of more surficial layers of metal grains reported by *Ireland et al.* (2005) are ^{17,18}O-enriched ($\Delta^{17}O_{SMOW} \sim +35‰$). The preservation of such anomalous oxygen component below the surface suggests solar wind implantation. The reasons for the discrepancy between the two data sets remain unclear. The ultimate test of both hypotheses will be provided by O-isotopic measurements of solar wind returned by the Genesis spacecraft.

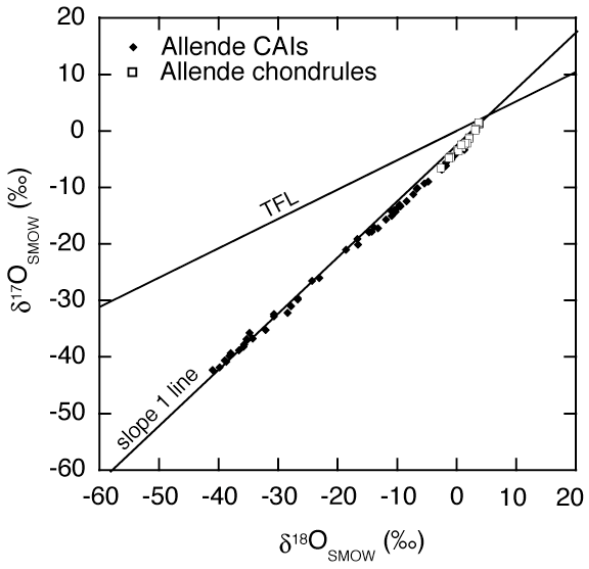

Fig. 2. Oxygen isotopic compositions of the refractory inclusions and chondrules in the CV3 Allende carbonaceous chondrite. Most refractory inclusions and chondrules deviate from the terrestrial fractionation line (TFL) and plot close to a line with a slope of 1. Data from *Clayton* (1993). Recently many new microanalysis data using SIMS and laser-ablation-MS have been reported (e.g., references in the text). The general distribution in the diagram remains nearly unaffected by the new data although understanding of the formation processes has been greatly developed by the new data.

6. ORIGIN OF OXYGEN ISOTOPIC ANOMALY IN THE SOLAR SYSTEM

Three different mechanisms have been proposed to explain the origins of the mass-independent O-isotopic fractionation with a slope of ~1 observed in chondrite components (Fig. 2).

6.1. Nucleosynthetic effects

According to the first group of hypotheses, the slope-1 line reflects an inherited O-isotopic heterogeneity in solar nebula materials (^{16}O-rich solids and ^{17,18}O-rich gas) resulting from either nucleosynthesis in stars (*Clayton et al.*, 1973) or from nuclear reactions that involve energetic particles from the proto-Sun or from galactic cosmic rays (*Lee*, 1978). However, since isotopic variations of other elements (e.g., Mg, Si, Ca, Ti) are much smaller and uncorrelated with the O-isotopic anomaly, this mechanism appears to be unlikely (*Clayton*, 1993). In addition, ^{16}O-rich presolar grains are exceptionally rare in meteorites

(*Nagashima et al.*, 2004; *Nittler*, 2003).

6.2. Chemical mass-independent fractionation effects during formation of solids

According to the second hypothesis, the slope-1 line resulted from chemical mass-independent fractionation effects similar to those observed in gas-phase O_3 production (*Thiemens and Heidenreich*, 1983). Some solid, terrestrial nitrates and sulphates possess mass-independent isotopic effects that have survived for at least 100 Myr (*Thiemens et al.*, 2001). Sulfur is now known to have preserved mass-independent isotopic effects on Earth for at least 3.8 Gyr (*Farquhar et al.*, 2000).

Because the solar nebula is too reducing for O_3 to be a significant component, *Thiemens* (1999, 2006) proposed that reactions involving symmetric components of silicate vapors such as $O + SiO \rightarrow SiO_2$ were responsible for the O-isotopic anomalies in chondrites. These molecules are vapor-phase precursors to minerals common in CAIs and chondrules. The analogous reaction $O + CO \rightarrow CO_2$ has been shown to yield a mass-independent fractionation signature. SiO_2 has its symmetry modified by substitution of ^{17}O or ^{18}O, as occurs for isotope substitution at the terminal oxygens of O_3. The same would also hold for reactions involving AlO, FeO, MgO, or CaO, all relevant nebular constituents. The chemical mechanism of mass-independent fractionation in O_3 is believed to be a preferential stabilization of the asymmetric isotopologue arising from a lack of intramolecular equilibrium in the symmetric isotopologue, referred to as an η-effect (*Gao et al.*, 2002). Although an η-effect could also occur during $SiO_{2(g)}$ formation, *Marcus* (2004) has argued that $O + SiO \rightarrow SiO_2$ in the inner gas phase solar nebula will be too slow by several orders of magnitude versus the reaction of O with H_2 to form H_2O. Instead, *Marcus* (2004) proposed that mass-independent fractionation occurred during SiO_2 formation on grain surface during CAI formation. This removes the spatial dependency and allows the reaction to occur anywhere in the nebula. It is known that O_3 formed on the walls of reaction vessels does not have a mass-independent fractionation signature, but how relevant that result is to SiO_2 formation, in which SiO is incorporated into the grain surface, is unclear. Experiments involving metal oxide reactions will be of importance in developing a model for the reactions in the nebula. The reactions of O + CO and OH +CO have been demonstrated to produce mass independent isotopic effects, consistent with the proposed role in the nebula via symmetry reactions.

A past limitation in model considerations has been the inability to define the role of the sun and photochemistry in the solar system. Recently, *Rai et al.* (2005) have reported mass-independent sulfur isotopic effects in four achondritic meteorite classes at the bulk level. The results appear consistent with a photochemical production, as observed in terrestrial Precambrian solids (*Farquhar et al.*, 2000). As shown in this paper, the only explanation that may account for these observations requires gas phase photochemistry of sulfur species. This requires photochemistry prior to condensation and incorporation into meteorites, directly implicating photochemistry in the nebula. This observation and photochemical requirement is consistent with both the symmetry (production of O atoms and OH radicals) and self-shielding models discussed in the following section.

6.3. Photochemical self-shielding effects

The third mechanism proposed for the mass-independent O-isotopic fractionation is photochemical self-shielding effects in CO. Self-shielding in O_2 was firstly considered as a possible solar nebular process (*Kitamura and Shimizu*, 1983; *Thiemens and Heidenreich*, 1983). It was shown later that trapping of photodissociated O by metal atoms, hydrogen, and O_2 is inefficient compared to O-isotopic exchange reactions in the solar nebula (*Navon and Wasserburg*, 1985). *Thiemens and Heidenreich* (1983) and *Navon and Wasserburg* (1985) proposed that self shielding in CO, as observed in astronomical environments, was responsible for production of the meteoritic isotopic anomalies.

The isotopically selective photolysis of CO has been well-known in the astronomical community for a long time (*Bally and Langer*, 1982, *van Dishoeck and Black*, 1988), and this mechanism has also been also suggested to explain the origin of the O-isotopic anomaly in meteorites and the evolution of O-isotopic compositions of the inner solar nebula (*Clayton*, 2002; *Lyons and Young*, 2005; *Yurimoto and Kuramoto*, 2004).

Three different astrophysical settings for CO self-shielding have been proposed to account for the solar system oxygen isotopic anomalies: the protosolar molecular cloud (*Yurimoto and Kuramoto*, 2004), the inner protoplanetary disk (*Clayton*, 2002) and the outer protoplanetary disk (*Lyons and Young*, 2005) (for details see sections 7 and 8). In all three cases it is assumed that the bulk O-isotopic composition of the protosolar molecular cloud, and, hence, the bulk composition of the Sun, is ^{16}O-rich; i.e., $^{17,18}O_{SMOW} = -50‰$. We note that this assumption is consistent with oxygen isotope measurements of solar wind by *Hashizume and Chaussidon* (2005), but is inconsistent with the results of *Ireland et al.* (2005). In the following discussion, it is convenient to use bulk composition of the molecular cloud as the new reference standard

($\delta^{17,18}O_{MC}$). In this case, $\delta^{17,18}O_{MC} = \delta^{17,18}O_{SMOW} + 50‰$.

7. SELF-SHIELDING OF CO IN MOLECULAR CLOUDS

Self-shielding effects of CO as a mechanism for O-isotopic fractionation were originally discussed in the context of molecular clouds by *Solomon and Klemperer* (1972). The self-shielding of CO is a process of isotope-selective photodissociation that occurs at far-ultraviolet (FUV) wavelengths from 91.3 nm to 107.6 nm. Because CO first goes to a bound excited state before dissociating (predissociation), the absorption spectrum of CO consists of many narrow lines. The wavelength of each line is determined by the specific vibrational and rotational levels involved, and is shifted when the mass of the molecules is changed as a result of an isotopic substitution. The absorption spectra of the various CO isotopologues do not overlap significantly, particularly at the low temperatures of molecular clouds. In the environment of molecular clouds, predissociation due to line spectrum absorption of UV photons is the dominant mechanism for photodissociation of CO (*Bally and Langer*, 1982; *Chu and Watson*, 1983; *Glassgold et al.*, 1985; *Marechal et al.*, 1997b; *van Dishoeck and Black*, 1988; *Warin et al.*, 1996). UV intensity at the wavelengths of dissociation lines for abundant $C^{16}O$ rapidly attenuates in the surface layer of a molecular cloud, because the cloud becomes optically thick in the lines of $C^{16}O$ after only short penetration depths. For less abundant $C^{17}O$ and $C^{18}O$, which have shifted absorption lines because of the differences in the vibrational-rotational energy levels, the attenuation is much slower. As a result, $C^{17}O$ and $C^{18}O$ are dissociated by UV photons even in a deep molecular cloud interior. This process results in selective enrichment of atomic oxygen in ^{17}O and ^{18}O.

Large mass-independent fractionation of oxygen isotopes resulting in $^{17,18}O$-depletion, i.e., ^{16}O-enrichment, in CO has been observed in a diffuse molecular cloud toward X Persei (*Sheffer et al.*, 2002), supporting the CO self-shielding hypothesis (Fig. 3).

Evidence for mass-independent fractionation of oxygen isotopes has also been observed in star-forming molecular clouds. Systematic observations of the variation of multiple minor CO isotopologues with dust column density have been reported for the IC 5146 dark cloud (Fig. 4). $^{13}CO/C^{18}O$ ratios in IC 5146 increase with decreasing visual extinction (*Av*) (Fig. 4) (*Lada et al.*, 1994). Because the $C^{18}O$ abundance is about 5 times lower than the ^{13}CO abundance, this trend indicates a selective UV photodissociation of $C^{18}O$ by self-shielding. It is also to be noted that the effect of selective photo-dissociation of ^{13}CO is diluted by exothermic ion molecule reaction $^{12}CO + {}^{13}C^{+} \rightarrow {}^{13}CO + {}^{12}C^{+}$, thereby ^{13}CO is expected to track fairly well the abundance of ^{12}CO, i.e. the $^{13}CO/^{12}CO$ ratio little fractionated in molecular clouds (e.g., *Warin et al.*, 1996). On the other hand, the $C^{18}O/C^{17}O$ ratios are nearly constant for all *Av* range from 0 to 40 mag, suggesting equal photodissociation efficiency for $C^{18}O$ and $C^{17}O$ (*Bergin et al.*, 2001). These results indicate that mass independent O-isotopic fractionation with $^{17,18}O$-depletion of CO occurs in IC 5146. Similar isotopic characteristics for ^{13}CO, $C^{17}O$ and $C^{18}O$ isotopologues have been observed in the ρ Oph dark cloud, the nearest low-mass star-forming region (*Wouterloot et al.*, 2005), and Orion molecular cloud (OCM1), an active high-mass star-forming region near to us (*White and Sandell*, 1995).

Based on these observations, we infer that mass-independent isotopic fractionation is a common feature of the diffuse, dark, and giant molecular clouds, and that most low- and high-mass stars probably formed from molecular clouds having mass-independent fractionation of CO. However, due to large uncertainties in the oxygen isotopic analysis, more precise measurements are necessary to state whether the effect is the requisite equal $^{17}O/^{18}O$ pattern required by current models. The isotopic fractionation factor associated with the actual photodissociation has not been measured in laboratory. Large mass dependent isotopic fractionations are known to occur in some photodissociation processes.

Because CO and atomic O are the dominant oxygen-bearing gas species in molecular clouds (*Marechal et al.*, 1997a), their isotopic fractionation caused by UV self-shielding may propagate to other O-bearing species. Water ice is the dominant O-bearing species among ices in molecular clouds (Fig. 5), where it nucleates and grows on silicate dust grains by surface hydrogenation reactions between atomic oxygen and hydrogen (*Aikawa et al.*, 2003; *Greenberg*, 1998). Therefore, O-isotopic compositions of H_2O ice should be close to those of gaseous atomic O; that is, enriched in ^{17}O and ^{18}O (*Yurimoto and Kuramoto*, 2004), assuming there are no large mass fractionation effects associated with the formation process. Water ice is observed in molecular clouds with $A_v > 3.2$; its abundance increases with increasing A_v (*Whittet et al.*, 2001).

In collapsing protostellar molecular cloud cores, most of the atomic O reacts to form H_2O ice, and CO becomes the dominant oxygen-bearing gas species within 10^5 years (*Bergin et al.*, 2000). In more evolved, cold molecular cloud cores, most CO could become frozen onto dust grains (*Aikawa et al.*, 2003). Because of the low temperature, O-isotopic exchange among CO gas, CO ice, and H_2O ice is insignificant, and the

evolved isotope fractionation of oxygen is preserved in each phase. Thus, O-isotopic compositions of CO and H_2O become depleted and enriched in $^{17,18}O$ with time, respectively.

Low-mass stars form by collapse of individual cores in a cold, dark cloud with $5< A_v <25$ and temperatures as low as ~10 K (*van Dishoeck et al.*, 1993). Under these conditions, a model simulating photochemical isotopic fractionation implies that the O-isotopic compositions ($\delta^{17,18}O_{MC}$) of H_2O ice and CO are in the range of +100 to +250‰ and -60 to -400‰, respectively (*Marechal et al.*, 1997b). These values are consistent with astronomical observations (*Ando et al.*, 2002; *Lada et al.*, 1994; *White and Sandell*, 1995, *Wouterloot et al.*, 2005).

For the protosolar molecular cloud, *Yurimoto and Kuramoto* (2004) assumed average $\delta^{17,18}O_{MC}$ values for silicates, H_2O ice, and CO of 0‰, +120‰, and -80‰, respectively (Fig. 6a). These values were chosen to be consistent with the astronomical studies and the relative oxygen abundances of silicates, H_2O ice, and CO (1 : 2 : 3) of a molecular cloud of solar bulk composition (*Greenberg*, 1998). The $^{17,18}O$-depleted compositions of primary solids and $^{17,18}O$-enriched nature of H_2O ice in the solar nebula are supported by meteoritic evidence (see section 3 for detail).

8. EVOLUTION OF PROTOPLANETARY DISKS AND OXYGEN ISOTOPES

8.1. Protoplanetary disk evolution

Protoplanetary disks form as a result of gravitational collapse of dense molecular cloud cores. Protoplanetary disks are evolving objects; the surface mass density and mass accretion rate both decrease as matter is accreted onto the star or photo-evaporated into interstellar space, and the disk outer edge expands (*Hartmann*, 2005). Temperatures in the inner disk regions depend on these accretion rates, but temperatures in the outer disk regions are nearly independent of accretion rate and are probably low enough that the primordial O-isotopic compositions of the molecular cloud components would have been preserved there in the absence of other effects. For instance, CO ice may sublime while preserving its O-isotopic composition (Fig. 6b). However, as material collapses from the protostellar molecular cloud into the disk, some of it passes through accretion shocks (*Chick and Cassen*, 1997) which may result in some isotopic re-equilibration of CO and H_2O and with other oxygen reservoirs (*Lyons and Young*, 2005).

During all early stages of nebula evolution, UV radiation from the central protostar and perhaps neighbouring massive stars (*Hester and Desch*, 2005) will be present – strongest at the innermost edge of the disk near the protostar, but also important in the low-density outer surfaces of the disk (*Adams et al.*, 2004). This irradiation may result in isotopic self-shielding effects in either or both places, as described below (see sections 8.2 and 8.3).

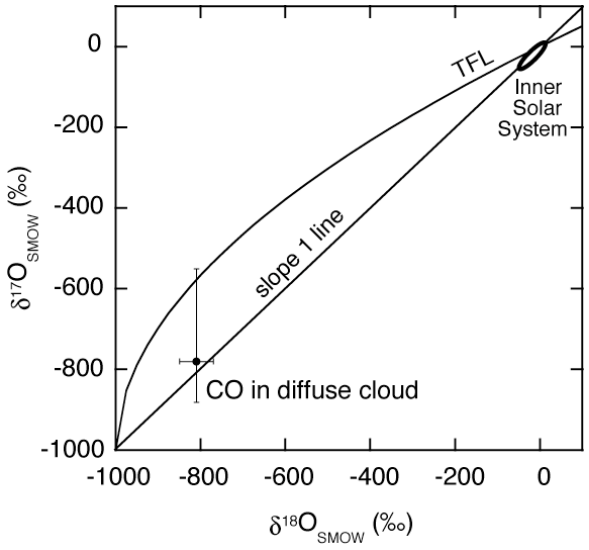

Fig. 3. Oxygen isotopic composition of CO in a diffuse molecular cloud towards X Persei. Data from *Sheffer et al*. (2002).

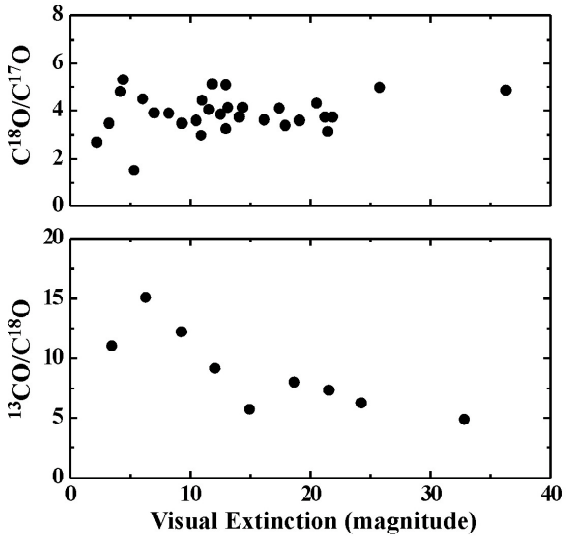

Fig. 4. Isotopic compositions of CO isotopologues in IC 5146 dark cloud. Data from *Lada et al*. (1994) and *Bergin et al*. (2001).

Astronomical observations set timescales for the evolution of disks (*Haisch et al.*, 2001; *Hartmann*, 2005), and absolute and relative chronologies of chondrite components provide constraints on the duration of the formation and thermal processing of solids in our own disk (*Amelin et al.*, 2002; *Baker et al.*, 2005; *Bizzarro et al.*, 2004; *Kita et al.*, 2005; *Krot et al.*,

2005b). These timescales are in general accord, lying in the range of 3-5 Myr for the duration of dust-rich disks.

Young disks undergo a *vigorously accreting stage* lasting < 1 Myr, characterized by accretion rates of several times 10^{-6} solar masses per year and temperatures in the innermost nebula hot enough to vaporize most silicates (*Cuzzi et al.*, 2005; *Muzerolle et al.*, 2003; *Woolum and Cassen*, 1999); this stage might be associated with Class 0 or even some Class I protostars. Most Class I objects are in the 1-5 Myr old range, and are accreting at lower rates (between 10^{-7} - 10^{-9} solar masses per year), with inner nebula temperatures cool enough for chondrules and other rock-forming minerals, but not water ice, to be solid. Water ice condenses only outside the snow line, a location that varies with model and with time as the nebula cools, but lies well outside the asteroid formation region for most of the evolution of the nebula in most models. Superimposed on this nebula gas density and temperature evolution is the transport of trace gases and solids by advection, diffusion, and gas drag migration, which changes the chemistry of the nebula over its lifetime. This evolution will depend on the intensity of turbulence, and turbulent diffusion, in the nebula – something that remains poorly understood but will be assumed here.

8.1.1. Disk evolution of solids and gas

Particles immersed in the disk have a relative motion against ambient gas, which rotates with a slightly slower speed than the Keplerian velocity due to the generally outward radial pressure gradient. The frictional loss of angular momentum due to their relative motion causes a drift of the dust grains toward the central star (*Weidenschilling*, 1977; for recent reviews see also *Cuzzi et al.*, 2005, *Cuzzi and Weidenschilling*, 2005, see the chapter by *Dominik et al.*). Solids probably can grow by coagulation into meter-sized particles that move rapidly inwards due to gas drag. Instead of being "lost into the sun" as sometimes assumed, particles migrate inward only until the temperature becomes high enough to evaporate them (Fig. 6e). If about 10% of the mass in solids is in the rapidly drifting meter-size range, material is carried inward across the snow line as solids faster than it can be removed as a vapor by the advection of the disk and diffusion of its vapor. The disk immediately inside the evaporation front thus becomes enhanced above solar in its vapor concentration, and as time goes on and the process continues, this enhancement spreads throughout the entire inner disk (Fig. 6e). This evaporation front effect occurs for any volatile, but silicates and water are especially interesting (*Cuzzi et al.*, 2003; *Cuzzi and Zahnle*, 2004).

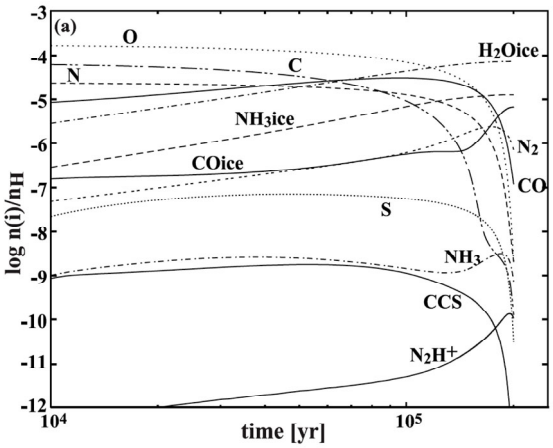

Fig. 5. Temporal variations of molecular abundances with grain-surface reactions. From *Aikawa et al.* (2003).

Here we focus on the water evaporation front as having direct relevance to O-isotope compositions and their variations with space and time. The most recent modeling of this process has been done by *Ciesla and Cuzzi* (2006), where a globally evolving disk is followed for several Myr, for a number of parameter choices. The surface density and temperature structure change consistently over the disk lifetime. As the gas disk evolves, the radial distribution of water solids and vapor evolves differently by transport, vaporization, condensation, accretion, and collisional destruction. Prior modeling by *Stepinski and Valageas* (1996) and *Kornet et al.* (2001) first showed these decoupling effects for the solids. The *Ciesla and Cuzzi* (2006) model considers four types of nebular materials: vapor, dust, migrators, and planetesimals. Vapor and dust (solid particles smaller than a meter) are transported by diffusion, which carries them either inward or outward along concentration gradients. Migrators represent the meter-sized rubble in the disk that drifts rapidly inward (~1 AU/century) because of gas drag. Planetesimals are larger objects (>1 km) which are massive enough to be unaffected by the gas in the disk and are immobile in the simulations. *Stevenson and Lunine* (1988) proposed that formation of immobile planetesimals outside the snowline served as a cold finger that could dry out the entire inner nebula; we now see that this is but one of several possible stages nebula water content can go through – perhaps the final stage.

Fig. 7 shows a schematic of the temporal and spatial evolution of the water content of the nebula, and Fig. 8 shows recent numerical model results from *Ciesla and Cuzzi* (2006). The numerical models show the enhanced water abundance propagating into the inner solar system (regime 2) on a timescale which is in good accord with simple diffusion and advection arguments (*Cuzzi and*

Zahnle, 2004).

The enrichment of the inner disk in water vapor decreases at later times (regime 3) because the growth of planetesimals prevents migrators from reaching the inner disk. Because vapor is not being supplied to the inner disk at such a rapid rate, diffusion of water vapor becomes the dominant transport mechanism. Vapor is thus carried outward where it condenses and is locked up on the immobile planetesimals outside the snow line. The concentration of vapor in the inner disk then decreases to less-than-solar values.

In an accretion disk, the coalescence of dust particles may be inhibited as a dust particle grows near the size comparable with the mean free path of nebular gas (e.g., *Sekiya and Takeda*, 2005) because collision velocity with smaller particles begins to rapidly increase. However, even mm-sized dust grains possibly migrate selectively enough to cause significant enrichment of water vapor in the inner disk when the disk mass accretion rate becomes lower than ~10^8 solar masses per year (*Kuramoto and Yurimoto*, 2005; *Yurimoto and Kuramoto*, 2004). In such a case, fluctuation of nebular accretion rate as expected from observation (e.g., *Calvet et al.*, 2000) would cause significant temporal variation of water vapor content and redox state in the innermost disk where refractory condensates are actively reprocessed (*Kuramoto and Yurimoto*, 2005).

8.2. Self-shielding in the inner disk

Because during the early stages of disk evolution, the central protostar provides a strong source of UV radiation, it was proposed that preferential photodissociation of $C^{17}O$ and $C^{18}O$, and formation of isotopically-heavy atomic oxygen, occurred at the innermost edge of the disk (*Clayton*, 2002). This scenario made use of the astrophysical setting of the X-wind model (*Shu et al.*, 2001; *Shu et al.*, 1996), suggesting that isotopically-heavy atomic oxygen produced this way was efficiently trapped in oxides, silicates, and H_2O vapor produced by oxidation of metallic elements and H_2 near the X-point, processed near the X-point to form chondrules, and launched by an X-wind to 1-3 AU from the proto-Sun, where together with matrix and refractory inclusions they accreted into chondrite parent asteroids. According to this model, refractory inclusions formed in a gas-depleted region of the disk inside the X-point, and hence largely preserved the initial, ^{16}O-rich isotopic composition of the primordial solids ($\delta^{17,18}O_{MC} = 0‰$). This model postulates that all solids in the inner Solar System were thermally processed through an X-region and attempts to unify the oxygen isotope photochemistry with the chemistry formation of

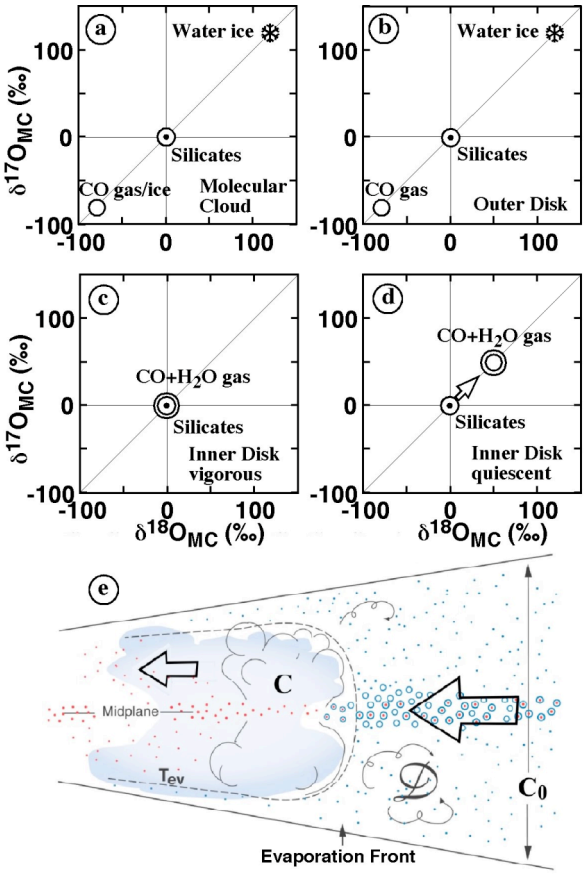

Fig. 6. (**a-d**) - Schematic diagrams of the evolution of O-isotopic compositions of the solar system from a protosolar molecular cloud (**a**) to the protoplanetary disk at different locations and various stages of its evolution: outer disk during vigorous and quiescent stages (**b**), vigorous inner disk (**c**), and quiescent inner disk (**d**) An arrow in (**d**) shows a direction of solid-gas equilibration. After *Yurimoto and Kuramoto* (2004). (**e**) - Sketch illustrating inwardly drifting water ice-rich material (circles) crossing water evaporation front (snow line) with midplane temperature T_{ev}; dots show the more refractory material (silicates, oxides, metal, sulfides, and organics). The large inward drift flux of water-ice-rich material cannot be offset by water removal processes until the concentration of the water vapor is much greater than its nominal solar value C_0. After *Cuzzi and Zahnle* (2004).

chondrules and CAIs (*Clayton*, 2002; *Shu et al.*, 1996). This model however does not account for the effect of isotopic exchange between the anomalous oxygen atom and CO, a limitation proposed by *Navon and Wasserburg* (1985).

There are several arguments against significant isotope-selective photodissociation of CO at the X-point. First, for the expected high gas temperatures of the innermost solar nebula (~1000-2000 K), H_2O is likely to

be present with a partial pressure comparable to CO although the ratio would be depend on the photodissociation rates of the molecules and collision rates of the photodissociated species at the X-point. H_2O is a continuum absorber and will diminish $C^{17}O$ and $C^{18}O$ dissociation in the region of $C^{16}O$ self-shielding (*Lyons and Young*, 2003). Second, at high temperatures band overlap occurs because of the increase in high-J rotational states, and because v > 0 ground state vibrational levels are populated. Both of these effects increase the likelihood of line overlap, which diminishes the effectiveness of CO self-shielding (*Navon and Wasserburg*, 1985). Third, the preservation of ^{17}O and ^{18}O-enrichment for H_2O near the X-point is problematic. The high temperatures at the innermost part of the disk facilitate reaction of C (either atomic or as C^+) with isotopically enriched H_2O, which erases the O-isotopic fractionation produced during CO self-shielding (*Lyons and Young*, 2003). Finally, the radial penetration depth of solar UV is extremely small, and it would be hard for chondrules to be produced sufficiently close to the protosun for them to benefit from any $^{17,18}O$ so released. In fact, *Muzerolle et al.* (2003) find that vigorously accreting stars vaporize essentially all solids (certainly all chondrules) out to distances of 0.07-0.54 AU, slightly far distant for an X-point-related self-shielding effect to be relevant. These arguments against CO self-shielding at the X-point are only semi-quantitative, and await a more complete assessment.

8.3. Self-shielding in the outer disk

During the early stages of star evolution, UV radiation from the central protostar and from neighbouring massive stars (if star formation occurs in an aggregate of at least ~ 100 stars) is expected to produce heavily-irradiated outer disk surfaces (*Adams et al.*, 2004). This irradiation may result in isotopic self-shielding effects in the surface skin layer of the disk. The isotopically heavy atomic oxygen (^{17}O and ^{18}O) is produced during photodissociation of $C^{17}O$ and $C^{18}O$, and is transferred to H_2O ice by the same process as described for molecular clouds (see section 7).

Surface self-shielding has been proposed in a photochemical model of a turbulent (α-disk) solar nebula (*Lyons and Young*, 2005). In this model FUV radiation was taken to be normal to the disk midplane, and a set of time-dependent chemical continuity equations was solved at a specified heliocentric distance and for a vertical eddy diffusion coefficient assumed to be equal to the turbulent viscosity, $\nu_t = \alpha c_s H$. The chemical network includes H-C-O species in a set of gas-phase, ion-molecule, and gas-grain reactions, in which all three isotopes of oxygen are explicitly computed. CO shielding functions from *van Dishoeck and Black* (1988) were used to compute the photolysis rates of CO isotopologues. Oxygen atoms liberated during CO photolysis form H_2O enriched in ^{17}O and ^{18}O by gas-grain reactions with H atoms. Fig. 9 shows

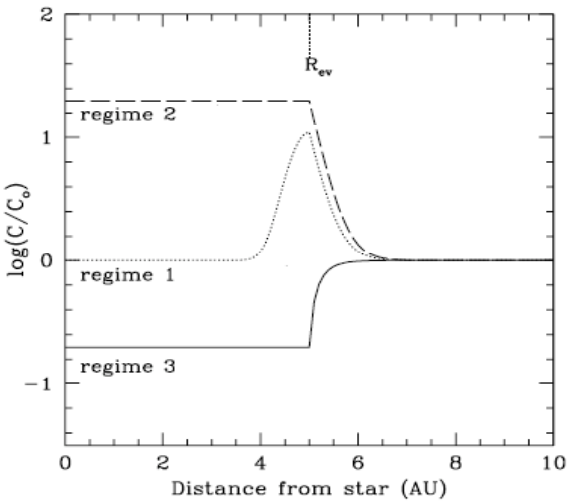

Fig. 7. Schematic of three regimes of the evolution of water vapor inside its evaporation front. An initial intense pulse is short-lived, and propagates throughout the inner solar system on a timescale of 10^5-10^6 years depending on nebula properties. Later on, after immobile planetesimals provide a cold sink outside the snowline, the inner nebula can be dried out. From simplified analytical models by *Cuzzi and Zahnle* (2004).

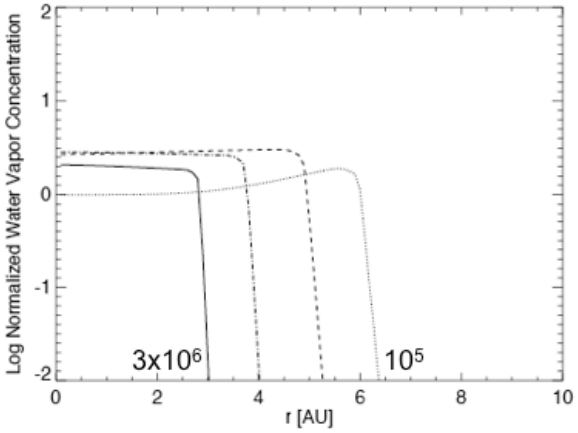

Fig. 8. Results from an evolving nebula model by *Ciesla and Cuzzi* (2006). The snowline moves to smaller radii with time as the nebula cools (water vapor abundance is shown at 10^5, 10^6, 2×10^6, and 3×10^6 years, respectively). This is typical of a range of models, most of which show water vapor enhancements reaching only a factor of several because of limits on how much icy material can migrate in from the outer solar system. This particular model has not reached regime 3 by the end of the simulation.

model results at 30 AU (midplane temperature = 51 K) for $\alpha = 10^{-2}$ and for a range of FUV enhancements above the local ISM FUV field. The shaded region shows the minimum initial nebular water $\Delta^{17}O_{SMOW}$ value necessary to account for the CAI slope-1 mixing line, as inferred from carbonaceous chondrites (*Clayton and Mayeda*, 1984; *Young*, 2001). A FUV flux enhancement factor of ~ 10^3 is needed for total nebular water (i.e., water produced as a result of CO photodissociation at the disk surface plus water inherited from the parent molecular cloud) at the midplane of the model to reach this range of $\Delta^{17}O$ values within a time << 1 Myr, the approximate minimum residence time for gas in the nebula. The radial motion of disk materials mentioned in section 8.1 should be incorporated in the future study.

Fig. 10 gives the time trajectory of total nebular water on a 3-isotope plot for the same FUV enhancement factor. The model slope is ~ 5 to 10% greater than the measured CAI mixing line due to self-shielding by $C^{18}O$. The model slope is reduced by ~ 5% when differential shielding by H_2 is accounted for in a particularly important band of CO for ^{17}O and ^{18}O formation [band 31 in *van Dishoeck and Black* (1988)], which yields better agreement with the meteorite data. Mass-dependent effects, which have not been included here, may also affect the model slope for nebular water. A distinct advantage of this model as compared to that of *Clayton* (2002) is that the low temperature kinetically quenches the isotopic exchange process. On the other hand, the high temperatures of *Clayton* (2002) reduce the magnitude of mass-dependent fractionation to 1-2‰, i.e., into the "noise".

8.4. Stages of disk evolution and oxygen isotopes

8.4.1. Vigorous early disk stage

The very early (Class 0) stage of nebula evolution, accompanied by vigorous accretion and high inner nebula temperatures, was fairly short (perhaps 10^5 years), so even if meter-sized particles had begun to form and drift radially, the water plume at the water evaporation front had not yet had time to propagate into the inner solar system. Thus, the mean O-isotopic composition of the gas in the inner part of the disk probably remained similar to the bulk O-isotopic composition of the protosolar molecular cloud ($\delta^{17,18}O_{MC}$ = 0‰; Fig. 6c). The earliest transient heating events in the inner solar nebula – formation of refractory inclusions (*Russell et al.*, 2005) – probably caused evaporation, condensation, and melting of the primordial dust in the presence of the nebular gas with $\delta^{17,18}O_{MC}$ = 0‰ during which the refractory inclusions would have formed and isotopically equilibrated with the nebular gas (*Itoh and Yurimoto*, 2003; *Krot et al.*, 2002). The similarity between the inferred ^{16}O-enriched composition of the Sun (*Hashizume and Chaussidon*, 2005) and the ^{16}O-rich compositions of the majority refractory in primitive chondrites is consistent with this scenario (*Yurimoto and Kuramoto*, 2004).

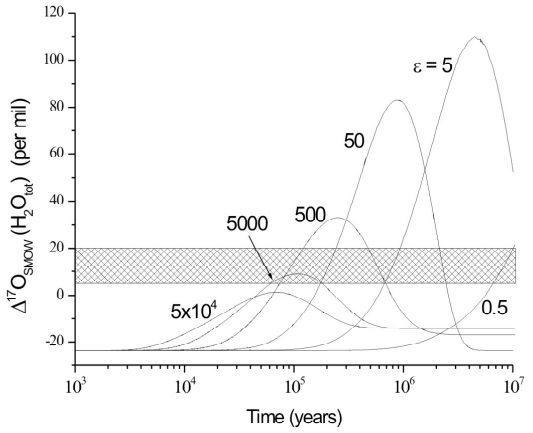

Fig. 9. Mass-independent fractionation signature ($\Delta^{17}O_{SMOW}$) predicted for total nebular water in an α-disk at 30 AU for a range of FUV fluxes. Total nebular water consists of water inherited from the protosolar molecular cloud and water produced as a result of isotope-selective photodissociation of CO in the nebula. O-isotopic composition of water in the protosolar molecular cloud is assumed to be equal to the bulk isotopic composition of the molecular cloud. Results are shown for $\alpha = 10^{-2}$ and for a FUV enhancement factor ε = 0.5 to 5×10^4 times the local interstellar medium FUV flux. The shaded region indicates the range of minimum $\Delta^{17}O$ inferred for nebular water from primitive meteorites (*Clayton and Mayeda*, 1984; *Young*, 2001). About 10^5 years are required to reach meteorite water values. From *Lyons and Young* (2005).

8.4.2. Towards quiescent disk stage

During the early stages of disk evolution, water transport is dominated by coagulation of sub-μm-sized dust into mm-to-meter-sized particles that then rapidly move inwards due to gas drag (*Weidenschilling*, 1977). This results in more icy material being carried inward across the snow line than can be removed by the advection of the disk and diffusion of water vapor (Fig. 6e; *Ciesla and Cuzzi*, 2006; *Cuzzi and Zahnle*, 2004). As a result, the inner disk immediately inside the snow line becomes enhanced in its water vapor concentration (Fig. 7). This inward flux continues as the water vapor is redistributed in the inner disk, resulting in a uniform enhancement of water vapor inside of the snow line, with the maximum enhancement reaching ~10×solar

(*Ciesla and Cuzzi*, 2006). If these inward migrating particles are enriched in isotopically heavy oxygen, as predicted in the self-shielding models of *Yurimoto and Kuramoto* (2004) and *Lyons and Young* (2005), the inner disk gas becomes increasingly enriched in $^{17,18}O$ over time (Fig. 6d) (*Yurimoto and Kuramoto*, 2004).

The degree of $^{17,18}O$-enrichment of the inner disk gas relative to the bulk O-isotopic composition of the protosolar molecular cloud is determined by the enrichment factor of water vapor and O-isotopic composition of CO and H_2O. If the average $\delta^{17,18}O_{MC}$ values for silicates, H_2O ice, and CO are 0‰, +120‰, and -80‰, and these are preserved in the outer disk (outside the snow line), the enrichment of the inner disk in water vapor by a factor of 3 relative solar abundance will produce gas with $\delta^{17,18}O_{MC}$ of +50‰, which is enough to explain the O-isotopic compositions of chondrules (Fig. 6d) (*Yurimoto and Kuramoto*, 2004). The $^{17,18}O$-rich signatures shown in chondrite components results from high temperature thermal processing in the $^{17,18}O$-rich disk gas, and of lower temperature aqueous alteration in the disk or on the planetesimal (the arrow of Fig. 6d). We note, however, that the presence of abundant crystalline silicates in anhydrous interplanetary dust particles, possibly of cometary origin (*Keller and Messenger*, 2005) and in cometary nuclei (*Harker et al.*, 2005), may indicate extensive thermal processing of primordial dust outside the snow line, possibly by shock waves (see the chapter by *Alexander et al.*; *Harker and Desch*, 2002). If this is the case, thermal processing of water ice and its isotopic equilibration with CO gas is expected. As a result, (*i*) it seems unlikely that the isotopic signature of H_2O and CO of the molecular cloud or of the outer disk will be entirely preserved, and (*ii*) higher enrichment factor of water vapor will be required to explain O-isotopic composition of chondrules.

The enrichment of the inner disk in water vapor decreases over time because growth of planetesimals outside the snow line prevents fast-moving, ice-rich rubble from drifting into the inner disk. Because vapor is not being supplied to the inner disk, diffusion carries water vapor outward where it condenses and is locked up in the immobile planetesimals. The concentration of water vapor in the inner disk then decreases over time (*Ciesla and Cuzzi*, 2006; *Stevenson and Lunine*, 1988). It may result in gradual enrichment of the inner disk gas in ^{16}O. It remains unclear whether any record of this fluctuating O-isotopic composition of the inner disk gas is preserved in chondritic components.

8.4.3. Planet accretion stage

Because the planets accrete during the quiescent disk stage (*Hayashi et al.*, 1985), each planet is expected to record the mean O-isotopic composition corresponding to the accretion regions of the disk. During the quiescent disk stage, the inner disk is probably enriched in ^{17}O and ^{18}O relative to bulk molecular cloud because of self-shielding and migration of H_2O-bearing icy particles across the snow line and thermal processing of dust in this $^{17,18}O$-enriched gas (Fig. 6d and see section 8.4.2). As a result, the inner solar system planets are expected to be rather uniformly $^{17,18}O$-rich, which is generally consistent with observations (Fig. 1a). For example, the difference in O-isotopic composition between the Earth and Mars (in terms of $\Delta^{17}O_{SMOW}$) is 0.3‰ (*Clayton*, 1993). Variations in O-isotopic compositions of meteorite parent asteroids are less than 10‰ (Fig. 1). The small differences observed among the meteorite parent asteroids could be explained by variations in time of asteroid accretion, incorporation of different amounts of non-vaporized water ice and solids with different degrees of the solid-gas equilibration etc., and the smaller variations between planets to the averaging associated with their growth.

Earth and Moon have identical (±0.016‰, $\Delta^{17}O$) O-isotopic compositions (Fig. 1a). There is a general consensus that Moon formed from hot mantle material thrown into orbit around Earth after the planet was hit by a Mars-sized impactor (e.g., *Cameron*, 1997). Theoretical work suggests that ~80% of the

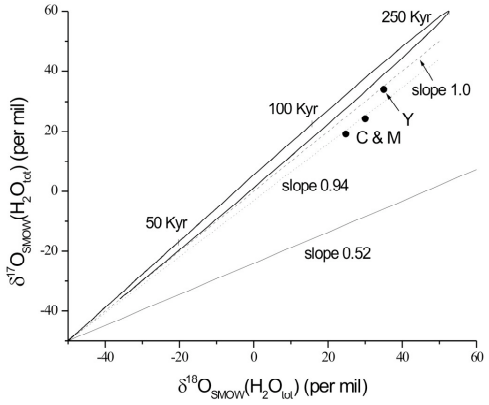

Fig. 10. Model prediction of the time trajectory of oxygen isotope ratios of total nebular water for the conditions of Figure 7 and for a FUV enhancement ε = 500. The points labeled 'C & M' and 'Y' correspond to the inferred nebular water values from *Clayton and Mayeda* (1984) and *Young* (2001), which lie on lines of slope 0.94 and 1.00, respectively. The model slope ($\delta^{17}O/\delta^{18}O$ ratio) is 5 to 10% higher than the slope inferred from primitive meteorites. From *Lyons and Young* (2005).

Moon-forming material comes from the impactor (*Canup and Asphaug*, 2001). As a result, the similarity in O-isotope composition between the Earth and the impactor has been interpreted as the formation at about the same heliocentric distances (*Wiechert et al.*, 2001). This conclusion, however, is inconsistent with the formation of the terrestrial planets by the stochastic collisions of embryos originating over much of the inner solar system (e.g., *Chambers*, 2001). It has therefore been proposed that the observed O-isotopic similarity between the Earth and Moon is due to O-isotopic exchange between the Earth's mantle and the circumterrestrial vapor-melt silicate disk that produced the Moon (*Pahlevan and Stevenson*, 2005)Additional work is needed to test this hypothesis.

In contrast to the relatively uniform ^{17,18}O-rich compositions of the inner solar system bodies at the quiescent disk stage, O-isotopic heterogeneity between H_2O and CO ices and silicates may be better preserved in the outer disk region (Fig. 6b). According to the standard core-accretion model of giant planet formation (*Pollack et al.*, 1996), run-away accretion of a solid core composed of ice and silicate dust is followed by accretion of disk gas. Because little fractionation is expected for H_2O ice and for silicate dust in the outer disk, the O-isotopic composition of the giant planet cores and icy planets would be $\delta^{17,18}O_{MC} \sim +70‰$, assuming solar proportions of ice and silicate dust. This value is also expected for Edgeworth-Kuiper-belt objects (KBOs) and comets.

Because the O-isotopic compositions of gas planets change with the ratio between captured gas and ice-dust core, observations of heavy elements in their envelopes would be an indicator of the ratio. The envelopes of gas planets are observed to be enriched in heavy elements relative to the solar composition (*Atreya et al.*, 1999, *Gautier and Owen*, 1989). Based on the observed enrichment of envelopes in heavy elements and the assumption that the O-isotopic compositions of silicate dust, H_2O ice and CO in the outer disk are similar to those in the protosolar molecular cloud, *Kuramoto and Yurimoto* (2005) predicted a relationship between the oxygen abundances and isotopic compositions of the giant planets (Fig. 11). We note that such a relationship would not expected if the molecular cloud O-isotopic signatures of these components were modified during the molecular cloud collapse, during transient heating events in the outer disk (e.g., *Harker and Desch*, 2002), or by self-shielding in the outer disk (*Lyons and Young*, 2005).

9. FUTURE WORK

The evolution scenario discussed in this paper implies that the oxygen isotopic anomaly occurs not only in the solar system but it is also ubiquitous in other protoplanetary disks and planetary systems. Therefore, a full understanding of oxygen isotopes in the early solar system will require further astronomical observations, experiments, and modelling. A direct high precision measurement of CO isotopologues in gas disks would confirm the presence of strong CO fractionation as predicted by self-shielding. Observation of a large oxygen isotope fractionation between gas-phase H_2O and CO in a disk would demonstrate isotopic partitioning of oxygen between these two key nebular species. ALMA may be capable of making these exceedingly difficult measurements. Key experiments needed are measurement of mass-independent fractionation in high-temperature silicate reactions (both gas-phase and surface) to verify the occurrence of mass-independent fractionation. Measurement of the $\delta^{17}O/\delta^{18}O$ ratio associated with isotope-selective photodissociation of CO are required at a geochemical (i.e., mass spectrometer) level of precision. Finally, modelling of oxygen isotopes in molecular clouds, collapsing cores, and protostellar nebulae, over temperatures ranging from 10 K to several 1000 K, will be needed to fully synthesize the meteorite and astronomical data.

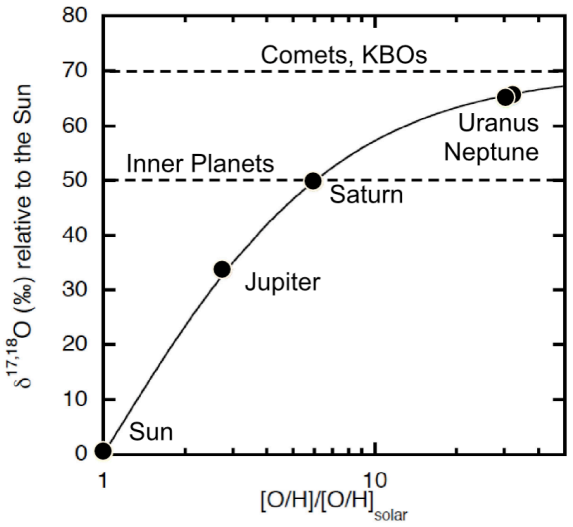

Fig. 11. Estimated O-isotopic compositions of giant planets and KBOs in the solar system.

Acknowledgements: This work was supported by Monkasho grants (H. Yurimoto, P. I.) and NASA grants NAG5-10610 (A. N. Krot, P. I.), NAG5-11591 (K. Keil, P. I.), and NASA's Planetary Geology and Geophysics and Origins of Solar Systems programs (J. N. Cuzzi, P. I.). JRL, ANK, and ERDS acknowledge support from the NASA Astrobiology Institute (NNA04CC08A (K. Meech, P.I.).

REFERENCES

Adams F. C., Hollenbach D., Laughlin G., and Gorti U. (2004) *Astrophy. J., 611*, 360-379.

Aikawa Y., Ohashi N., and Herbst E. (2003) *Astrophys. J., 593*, 906-924.

Aleon J., Krot A. N., and McKeegan K. D. (2002) *Meteorit. Planet. Sci., 37*, 1729-1755.

Aleon J., Krot A. N., McKeegan K. D., MacPherson G. J., and Ulyanov A. A. (2005a) *Meteorit. Planet. Sci., 40*, 1043-1058.

Aleon J., Robert F., Duprat J., and Derenne S. (2005b) *Nature, 437*, 385-388.

Amelin Y., Krot A. N., Hutcheon I. D., and Ulyanov A. A. (2002) *Science, 297*, 1678-1683.

Ando M., Nagata T., Sato S., Mizuno N., Mizuno A., et al. (2002) *Astrophys. J., 574*, 187-197.

Atreya S. K., Wong M. H., Owen T. C., Mahaffy P. R., Niemann H. B., et al. (1999) *Planet. Space Sci., 47*, 1243-1262

Baker J., Bizzarro M., Wittig N., Connelly J., and Haack H. (2005) *Nature, 436*, 1127-1131.

Bally J. and Langer W. D. (1982) *Astrophys. J., 255*, 143-148.

Bergin E. A., Ciardi D. R., Lada C. J., Alves J., and Lada E. A. (2001) *Astrophys. J., 557*, 209-225

Bergin E. A., Melnick G. J., Stauffer J. R., Ashby M. L. N., Chin G., et al. (2000) *Astrophys. J., 539*, L129-L132.

Bizzarro M., Baker J. A., and Haack H. (2004) *Nature, 431*, 275-278

Bland P. A., Rost D., Vicenzi E. P., Stadermann F. J., Floss C., et al. (2005) *Lunar Planet. Sci., XXXVI*, #1841.

Brearley A. J. (1996) In *Chondrules and the protoplanetary disk* (R. H. Hewins, R. H. Jones and E. R. D. Scott, eds.), pp. 137-151. Cambridge Univ. Press, Cambridge.

Calvet N., Hartmann L., and Strom S. E. (2000) In *Protostars and Planets IV* (V. Mannings, A. P. Boss and S. S. Russell, eds.), pp. 377-399. Univ. of Arizona, Tucson.

Cameron A. G. W. (1997) *Icarus, 126*, 126-137.

Canup R. M., and Asphaug E. (2001) *Nature, 412*, 708-712.

Chambers J. (2001) *Icarus, 152*, 205-224.

Chick K. M, and Cassen P. M. (1997) *Astrophys. J., 477*, 398-409.

Choi B. –G., McKeegan K. D., Krot A. N., and Wasson J. T. (1998) *Nature, 392*, 577 – 579.

Chu Y. –H., and Watson W. D. (1983) *Astrophys. J., 267*, 151-155.

Ciesla F. J., and Cuzzi J. N. (2006) *Icarus,* in press.

Clayton D. D., and Nittler L. R. (2004) *Ann. Rev. Astron. Astrophys., 42*, 39-78.

Clayton R. N. (1993) *Annu. Rev. Earth Planet. Sci., 21*, 115-149.

Clayton R. N. (2002) *Nature, 415*, 860-861.

Clayton R. N., Grossman L., and Mayeda T. K. (1973) *Science, 182*, 485-488.

Clayton R. N., and Mayeda T. K. (1984) *Earth Planet. Sci. Lett*., *67*, 151-161.

Clayton R. N., and Mayeda T. K. (1996) *Geochim. Cosmochim. Acta, 60*, 1999-2018.

Clayton R. N., and Mayeda T. K. (1999) *Geochim. Cosmochim. Acta, 63*, 2089-2104.

Cuzzi J. N., Davis A., and Dobrovolskis A. (2003) *Icarus, 166*, 385-402.

Cuzzi J. N., Petaev M., Scott E. R. D., and Ciesla F. (2005) In *Chondrites and the Protoplanetary Disk* (A. N. Krot, E. R. D. Scott, and B. Reipurth, eds.), pp. 732-773.

Cuzzi J. N., and Weidenschilling S. J. (2005) In *Meteorites and the Early Solar System, II* (D. Lauretta, L. A. Leshin, and H. McSween, eds.), in press.

Cuzzi J. N., and Zahnle K. J. (2004) *Astrophys. J., 614*, 490-496.

Desch S. J., and Connolly H. C. (2002) *Meteorit. Planet. Sci., 37*, 183-207.

Fahey A. J., Goswami J. N., McKeegan K. D., and Zinner E. K. (1987) *Astrophys. J., 231*, L91-L95.

Farquhar J., Bao H., and Thiemens M. H. (2000) *Science, 289*, 756-758.

Gao Y. Q., Chen W. –C., and Marcus R. A. (2002) *J. Chem. Phys., 117*, 1536-1543.

Gautier D., and Owen T. (1989) In *Origin and evolution of planetary and satellite atmospheres* (S. K. Atreya, J. B. Pollack and M. S. Matthews, eds.), pp. 487-512. Univ. of Arizona, Tucson.

Glassgold A. E., Huggins P. J., and Langer W. D. (1985) *Astrophys. J., 290*, 615-626.

Goswami J. N., Marhas K. K., and Sahijpal S. (2001) *Astrophys. J., 549*, 1151-1159.

Greenberg J. M. (1998) *Astron. Astrophys., 330*, 375-380.

Greenwood R. C., Franchi I. A., Jambon A., and Buchanan P. C. (2005) *Nature, 435*, 916-918.

Haisch K. E., Greene T. P., Barsony M., and Ressler M. (2001) *Astrophys. J., 553*, L153-L156.

Harker D. E., and Desch S. J. (2002) *Astrophys. J., 565*, L109-L112.

Harker D. E., Woodward C. E., and Wooden D. H. (2005) *Science, 310*, 278-280.

Hartmann L. (2005) In *Chondrites and the Protoplanetary Disk* (A. N. Krot, E. R. D. Scott and B. Reipurth, eds), pp. 131-144. ASP Conference

Series.
Hashizume K., and Chaussidon M. (2005) *Nature, 434*, 619-622.
Hayashi C., Nakazawa K., and Nakagawa Y. (1985) In *Protostars and Plotoplanets II* (D. C. Black and M. S. Matthews, eds.), pp. 1100-1153. Univ. of Arizona.
Hester J. J., and Desch S. J. (2005) In *Chondrites and the Protoplanetary Disk* (A. N. Krot, E. R. D Scott and B. Reipurth, eds.), pp. 107-131.
Hewins R. H., Connolly H. C., Lofgren G. E., and Libourel G. (2005) In *Chondrites and the Protoplanetary Disk* (A. N. Krot, E. R. D. Scott and B. Reipurth, eds.), pp. 286-317.
Ireland T. R., Holden P., and Norman M. D. (2005) *Lunar Planet. Sci., XXXVI*, #1572.
Itoh S., Kojima H., and Yurimoto H. (2004) *Geochim. Cosmochim. Acta, 68*, 183-194.
Itoh S., and Yurimoto H. (2003) *Nature, 423*, 728-731.
Jones R. H., Grossman G. N., and Rubin A. E. (2005) In *Chondrites and the Protoplanetary Disk* (A. N. Krot, E. R. D. Scott and B. Reipurth, eds.), pp. 251-286.
Keller L. P., and Messenger S. (2005) In *Chondrites and the Protoplanetary Disk* (A. N. Krot, E. R. D. Scott and B. Reipurth, eds.), pp. 657-668.
Kita N. T., Huss G. R., Tachibana S., Amelin Y., Nyquist L. E., and Hutcheon I. D. (2005) In *Chondrites and the Protoplanetary Disk* (A. N. Krot, E. R. D. Scott and B. Reipurth, eds.), pp. 558-588.
Kitamura Y, and Shimizu M. (1983) *The Moon and the Planets, 29*, 199-202.
Kobayashi S., Imai H., Yurimoto H. (2003) *Geochem. J., 37*, 663-669.
Kornet K., Stepinski T. F., Różyczka M. (2001) *Astron. Astrophys., 378*, 180-191.
Krot A. N., Amelin Y., Cassen P., Meibom A. (2005a) *Nature, 436*, 989-992.
Krot A. N., Hutcheon I. D., Yurimoto H., Cuzzi J. N., McKeegan K. D., et al. (2005b) *Astrophys. J., 622*, 1333-1342.
Krot A. N., Libourel G., Chaussidon M. (2006) *Geochim. Cosmochim. Acta,* in press.
Krot A. N., McKeegan K. D., Leshin L. A., MacPherson G. J., and Scott E. R. D. (2002) *Science, 295*, 1051-1054.
Krot A. N., Yurimoto H., Hutcheon I. D., MacPherson G. J. (2005c) *Nature, 434*, 998-1001.
Kunihiro T., Nagashima K., and Yurimoto H. (2005) *Geochim. Cosmochim. Acta, 69*, 763-773.
Kuramoto K., and Yurimoto H. (2005) In *Chondrites and the Protoplanetary Disk* (A. N. Krot, E. R. D. Scott and B. Reipurth, eds.), pp. 181-192. ASP Conference Series.
Lada C. J., Lada E. A., Clemens D. P., and Bally J. (1994) *Astrophys. J., 429*, 694-709.
Lee T. (1978) *Astrophys. J., 224*, 217-226.
Lee T., Shen J. J. (2001) *Meteorit. Planet. Sci., 36*, A111.
Lyons J. R., and Young E. D. (2003) *Lunar Planet. Sci., XXXIV*, 1981.
Lyons J. R., and Young E. D. (2005) *Nature, 435*, 317-320.
MacPherson G. J., Simon S. B., Davis A. M., Grossman L., and Krot A. N. (2005) In *Chondrites and the Protoplanetary Disk* (A. N. Krot, E. R. D. Scott and B. Reipurth, eds.), pp. 225-250.
Marcus R. A. (2004) *J. Chem. Phys., 121*, 8201-8211.
Marechal P., Viala Y. P., and Benayoun J. J. (1997a) *Astron. Astrophys., 324*, 221-236.
Marechal P., Viala Y. P., and Pagani L. (1997b) *Astron. Astrophys., 328*, 617-627.
Maruyama S., Yurimoto H., and Sueno S. (1999) *Earth Planet. Sci. Lett., 169*, 165-171.
McKeegan K. D., and Leshin L. A. (2001) In *Stable Isotope Geochemistry* (J. W. Valley and D. R. Cole, eds.), pp. 279-318. Reviews in Mineralogy and Geochemistry, vol. 43.
Muzerolle J., Calvet N., Hartmann L., and D'Alessio P. (2003) *Astrophys. J., 597*, L149-L152.
Nagashima K., Krot A. N., and Yurimoto H. (2004) *Nature, 428*, 921-924.
Navon O., and Wasserburg G. J. (1985) *Earth Planet. Sci. Lett., 73*, 1-16.
Nittler L. R. (2003) *Earth Planet. Sci. Lett., 209*, 259-273.
Nittler L. R., Alexander C. M. Od., Wang J., and Gao X. (1998) *Nature, 393*, 222.
Nittler L. R., Alexander C. M. Od., Gao X., Walker R. M., and Zinner E. (1997) *Astrophys. J., 483*, 475-495.
Pahlevan K., and Stevenson D. J. (2005) *Lunar Planet. Sci., XXXVI*, #2382.
Pollack J. B., Hubickyj O., Bodenheimer P., Lissauer J. J., Podolak M., and Greenzweig Y. (1996) *Icarus, 124*, 62–85.
Rai V. K., Jackson T. L., and Thiemens M. H. (2005) *Science, 309*, 1062-1065.
Russell S. S., Krot A. N., Huss G. R., Keil K., Itoh S., et al. (2005) In *Chondrites and the Protoplanetary Disk* (A. N. Krot, E. R. D. Scott and B. Reipurth, eds.), pp. 317-350. ASP Conference Series.
Scott E. R. D., and Krot A. N. (2001) *Meteorit. Planet. Sci., 36*, 1307-1319.
Scott E. R. D., and Krot A. N. (2003) In *Meteorites, Comets and Planets* (A. M. Davis, eds.), pp. 143-200. Elsevier, Oxford.
Sekiya M., and Takeda H. (2005) *Icarus, 176*, 220-223.
Sheffer Y., Lambert D. L., and Federman S. R. (2002)

Astrophys. J., 574, L171-L174.
Shu F. H., Shang H., Gounelle M., Glassgold A. E., Lee T. (2001) *Astrophys. J., 548*, 1029-1050.
Shu F. H., Shang H., and Lee T. (1996) *Science, 271*, 1545-1552.
Solomon P. M., and Klemperer W. (1972) *Astrophys. J., 178*, 389-422.
Stepinski T. F., and Valageas P. (1996) *Astron. Astrophys., 309*, 301-312.
Stevenson D. J., and Lunine J. I. (1988) *Icarus, 75*, 146-155.
Thiemens M. H. (1999) *Science, 283*, 341-345.
Thiemens M. H. (2006) *Annu. Rev. Earth Planet Sci.,* in press.
Thiemens M. H., Heidenreich J. E. (1983) *Science, 219*, 1073-1075.
Thiemens M. H., Savarino J., Farquhar J., and Bao H. (2001) *Accounts. Chem. Res., 34*, 645-652.
van Dishoeck E. F., and Black J. H. (1988) *Astrophys. J., 334*, 771-802.
van Dishoeck E. F., Blake G. A., Draine B. T., and Lunine J. I. (1993) In *Protostars and Planets III* (E. Levy and J. I. Lunine, eds.), pp. 163-241. Univ. of Arozona, Tucson.
Warin S., Benayoun J. J., and Viala Y. P. (1996) *Astron. Astrophys., 308*, 535-64
Weidenschilling S. J. (1977) *Mon. Not. Roy. Astr. Soc., 180*, 57-70.
White G. J., and Sandell G. (1995) *Astron. Astrophys., 299*, 179-192.
Whittet D. C. B., Gerakines P. A., Hough J. H., and Shenoy S. S. (2001) *Astrophys. J., 547*, 872-884.
Wiechert U., Halliday A. N., Lee D. –C., Snyder G. A., Taylor L. A., and Rumble D. (2001) *Science, 294*, 345-348.
Wood J. A. (1998) *Astrophys. J., 503*, L101-L104.
Wood J. A. (2004) *Geochim. Cosmochim. Acta, 68*, 4007-4021.
Woolum D. S., and Cassen P. (1999) *Meteorit Planet Sci., 34*, 897-907.
Wouterloot J. G. A., Brand J., and Henkel C. (2005) *Astron. Astrophys., 430*, 549-560.
Young E. D. (2001) *Phil. Tran. R. Soc. Lond. A, 359*, 2095-2110.
Young E. D., Simon J. I., Galy A., Russell S. S., Tonui E., and Lovera O. (2005) *Science, 308*, 223-227.
Yu Y., Hewins R. H., Clayton R. N., and Mayeda T. K. (1995) *Geochim. Cosmochim. Acta, 59*, 2095-2104.
Yurimoto H., and Kuramoto K. (2004) *Science, 305*, 1763-1766.